Cell

AKT/FOXO Signaling Enforces Reversible Differentiation Blockade in Myeloid Leukemias

Stephen M. Sykes,[1,2] Steven W. Lane,[3,8] Lars Bullinger,[6] Demetrios Kalaitzidis,[3] Rushdia Yusuf,[1,2] Borja Saez,[1,2] Francesca Ferraro,[1,2] Francois Mercier,[1,2] Harshabad Singh,[1] Kristina M. Brumme,[3] Sanket S. Acharya,[1,2] Claudia Scholl,[6] Zuzana Tothova,[4] Eyal C. Attar,[1] Stefan Fröhling,[6] Ronald A. DePinho,[5,9] D. Gary Gilliland,[7] Scott A. Armstrong,[3] and David T. Scadden[1,2,*]

[1]Center for Regenerative Medicine and Cancer Center, Massachusetts General Hospital, Boston, MA 02114, USA
[2]Department of Stem Cell and Regenerative Biology, Harvard University, Cambridge, MA 02138, USA
[3]Division of Hematology/Oncology, Children's Hospital of Boston, Harvard Medical School, Boston, MA 02115, USA
[4]Brigham and Women's Hospital, Harvard Medical School, Boston, MA 02115, USA
[5]Belfer Institute for Applied Cancer Science, Departments of Medical Oncology, Medicine, and Genetics, Dana-Farber Cancer Institute, Harvard Medical School, Boston, MA 02115, USA
[6]Department of Internal Medicine III, University Hospital of Ulm, Ulm 89081, Germany
[7]Merck Research Laboratories, North Wales, PA 19454, USA
[8]Present address: Queensland Institute of Medical Research, Brisbane 4006, Australia
[9]Present address: Division of Cancer Medicine, The University of Texas MD Anderson Cancer Center, Houston, TX 77030, USA
*Correspondence: dscadden@mgh.harvard.edu
DOI 10.1016/j.cell.2011.07.032

SUMMARY

AKT activation is associated with many malignancies, where AKT acts, in part, by inhibiting FOXO tumor suppressors. We show a converse role for AKT/FOXOs in acute myeloid leukemia (AML). Rather than decreased FOXO activity, we observed that FOXOs are active in ∼40% of AML patient samples regardless of genetic subtype. We also observe this activity in human MLL-AF9 leukemia allele-induced AML in mice, where either activation of Akt or compound deletion of *FoxO1/3/4* reduced leukemic cell growth, with the latter markedly diminishing leukemia-initiating cell (LIC) function in vivo and improving animal survival. FOXO inhibition resulted in myeloid maturation and subsequent AML cell death. FOXO activation inversely correlated with JNK/c-JUN signaling, and leukemic cells resistant to FOXO inhibition responded to JNK inhibition. These data reveal a molecular role for AKT/FOXO and JNK/c-JUN in maintaining a differentiation blockade that can be targeted to inhibit leukemias with a range of genetic lesions.

INTRODUCTION

The serine/threonine kinase AKT is a highly conserved central regulator of growth-promoting signals in multiple cell types. Deregulation of AKT has been associated with multiple human diseases including a wide variety of cancers (Altomare and Testa, 2005; Nicholson and Anderson, 2002). AKT functions by phosphorylating and inactivating substrates that antagonize

cell growth and survival, including PRAS40, GSK-3β, TSC2, BAD, and FOXOs (Brunet et al., 1999; Cross et al., 1995; Datta et al., 1997; del Peso et al., 1997; Inoki et al., 2002; Kops et al., 1999; Sancak et al., 2007). The kinase activity and substrate selectivity of AKT are principally controlled by phosphorylation of threonine 308 (pAKT^{Thr308}) and serine 473 (pAKT^{Ser473}) (Alessi et al., 1996). pAKT^{Ser473} is dispensable for AKT-mediated phosphorylation of TSC2 and GSK-3β, whereas pAKT^{Ser473} is required for phosphorylation and inactivation of the FOXOs (Guertin et al., 2006).

Direct mutations in components of the PI3K signaling pathway are rarely observed in human AML; however, elevated AKT phosphorylation has been observed in ∼50% (Park et al., 2010). pAKT^{Thr308} was shown to confer a poor prognosis in AML (Gallay et al., 2009), whereas pAKT^{Ser473} correlates with a favorable response to chemotherapy (Tamburini et al., 2007). In mouse models, constitutive activation of Akt or deletion of *Pten*, which suppresses Akt signaling, leads to myeloid or lymphoid neoplasia (Kharas et al., 2010b; Yilmaz et al., 2006). Collectively, these observations have supported the general concept that activated AKT signaling is associated with hematopoietic malignancies.

The FOXO family of transcription factors comprises four highly related members—FOXO1, FOXO3, FOXO4, and FOXO6—that are direct downstream targets of AKT (Arden, 2006; Brunet et al., 1999; Kops et al., 1999; Fu and Tindall, 2008). In the absence of active AKT, FOXOs localize to the nucleus where they regulate the transcription of genes involved in cell-cycle arrest, apoptosis, and reactive oxygen species (ROS) detoxification. Paradoxically, although FOXOs are primarily known as tumor suppressors, high FOXO3 expression is associated with adverse prognosis in AMLs exhibiting normal cytogenetics (Santamaría et al., 2009). Furthermore, genetic ablation of *FoxO3*

reduced disease burden in a murine model of chronic myeloid leukemia (CML) (Naka et al., 2010).

AMLs are genetically heterogeneous malignant neoplasms that have a low survival rate (Fröhling et al., 2005). AML prognosis is dependent on the cytogenetic and molecular profiles of AML cells (Armstrong et al., 2003; Dash and Gilliland, 2001; Döhner et al., 2010). The genetic and molecular diversity observed in AML has made the development of universal or broad AML-targeted therapies very difficult. Thus, investigation of the molecular signatures that separate AMLs into larger, more discrete groups is needed to develop more general and effective therapies.

We used human samples to assess the potential for AKT/FOXO signaling to divide AML into broad groups, and we used both an established murine model and human AML cells to define whether targeting AKT/FOXO could affect disease. We unexpectedly observed that low levels of AKT activity associated with elevated levels of FOXOs are required to maintain the function and immature state of leukemia-initiating cells (LICs). Furthermore, depletion of FOXO3 promoted differentiation and apoptosis of human myeloid leukemia cells. These data reveal an unrecognized role of the AKT/FOXO signaling pathway in the regulation and maintenance of AML that runs counter to the established roles of AKT/FOXO signaling in human cancer. Finally, we also observed that inhibition of FOXO, either directly or via AKT activation, stimulates the JNK/c-JUN pathway, which suppresses AML cell apoptosis. These findings provide unique molecular insights into how growth-control pathway perturbation can participate in malignancy and identify specific molecular targets for differentiation-inducing approaches to a large proportion of myeloid leukemias.

RESULTS

AKT Activity Is Diminished in MLL-AF9 CD34$^+$ Myeloid Progenitors

Because specific modifications of AKT confer distinct clinical outcomes of human AML (Gallay et al., 2009; Park et al., 2010; Tamburini et al., 2007), we examined Akt status in a murine model of MLL-AF9-induced myeloid leukemia that closely phenocopies human AML (Krivtsov et al., 2006). In this model, the L-GMP (leukemia-granulocyte macrophage progenitor) cell population, which shares the same immunophenotype of GMPs (lineage^{low}, cKit^{high}, Sca-1$^-$, FcγRII/III$^+$, CD34$^+$), is enriched for LIC activity. Akt phosphorylation was assessed by flow cytometry in cells from healthy and MLL-AF9 leukemic mice. Normal myeloid progenitors displayed a robust increase in both pAkt^{Ser473} and pAkt^{Thr308} (Figure 1A and Figure S1A available online); however, leukemic progenitors (enriched for L-GMPs) exhibited markedly reduced pAkt^{Ser473} and pAkt^{Thr308} in response to stimulation, indicating attenuated Akt activation (Figure 1A and Figure S1A). Cells were further evaluated for serine 235/236 phosphorylation of ribosomal S6 (pS6$^{Ser235/236}$), a downstream effector of AKT signaling (Burgering and Coffer, 1995). Normal CD34$^+$ cells showed strong induction of pS6$^{Ser235/236}$ (Figure S1B), whereas CD34$^+$ leukemic progenitors had a blunted pS6$^{Ser235/236}$ response, further demonstrating that Akt activity is diminished in MLL-AF9 LIC-enriched populations (Figure S1B).

Constitutive Activation of Akt Promotes Myeloid Differentiation and Apoptosis of Murine AML Cells

The diminished Akt activity in MLL-AF9-driven LICs and BCR-ABL-positive LICs (Naka et al., 2010) prompted us to determine the biological consequences of enforcing Akt activity in MLL-AF9-positive AML cells. To that end, bone marrow (BM) cells from MLL-AF9 leukemic mice were adapted to liquid culture and infected with recombinant retroviruses expressing a constitutively active form of Akt (myr-Akt). Cells expressing myr-Akt had markedly impaired proliferation compared to control-infected cells (Figure 1B), consistent with previous reports (Wang et al., 2008). Ablation of *Pten* (an inhibitor of Akt signaling) in the murine hematopoietic system results in the rapid onset of myeloid and/or lymphoid neoplasia (Lee et al., 2010; Yilmaz et al., 2006). Within this model, leukemogenesis is largely dependent on mammalian target of rapamycin (mTor) signaling, as rapamycin markedly delays disease onset (Yilmaz et al., 2006). Enforced expression of myr-Akt strongly increased the phosphorylation of mTor substrates (Figure S1D). However, treatment of myr-Akt-expressing AML cells with effective concentrations of rapamycin did not completely rescue the cell growth defect (Figure 1B and Figure S1C). Although these results do not exclude a role for mTor signaling, they do suggest that additional mechanisms might contribute to the cell growth defect associated with myr-Akt expression in murine AML cells.

Expression of myr-Akt in normal bone marrow reduces the self-renewal properties of normal hematopoietic stem and progenitor cells (HSPCs) and promotes myeloid maturation (Kharas et al., 2010b). Therefore, we examined whether myr-Akt expression was inhibiting AML cell growth by promoting myeloid maturation. myr-Akt cells displayed increased forward and side scatter by cytometry, consistent with mature myeloid cells (Figure S1E). Further, mature myeloid cell markers (CD11b) were higher on myr-Akt cells (Figure 1C), and myr-Akt cells exhibited morphological changes of myeloid maturation including reduced nucleoli, increased cytoplasmic volume, granule formation, and condensed chromatin (Figure 1D). Finally, myr-Akt cells acquired the ability to engulf fluorescent-labeled bacterial peptides, confirming the myr-Akt-directed maturation of leukemic blasts into functional myeloid cells with the capacity for phagocytosis (Figures 1E and 1F).

Upon completion of myelopoiesis, mature myelocytes have a limited life span in the peripheral blood. Therefore, we evaluated whether myr-Akt-induced maturation of myeloid cells is accompanied by increased cell death. Apoptosis was increased in myr-Akt myeloid cells (Figure 1G). Maturation-related death mediated by myr-Akt occurred in the presence of rapamycin, suggesting that Akt utilizes pathways other than mTor activation for myeloid maturation (Figures 1C–1F). Together, these results suggest that LICs within this model maintain low levels of Akt activity to preserve an immature cell state by preventing differentiation and death.

FoxOs Are Active in Murine MLL-AF9 L-GMPs

FoxOs play central roles in regulating normal hematopoiesis and are integral mediators of Akt's actions in cellular growth and survival (Fu and Tindall, 2008; Miyamoto et al., 2007; Tothova et al., 2007; Yalcin et al., 2008). We evaluated FoxO activity in
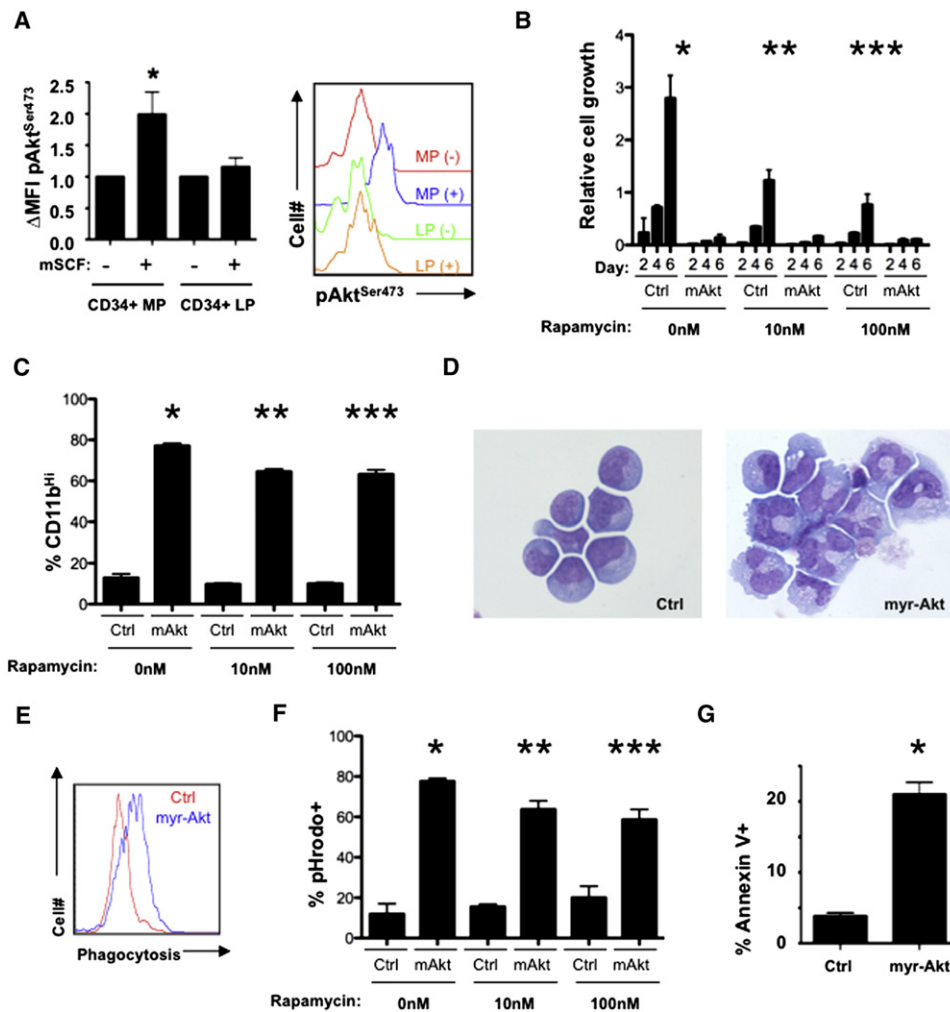
Figure 1. Constitutive Akt Activation Promotes Myeloid Maturation and Apoptosis of Leukemic Cells

(A) Lineage^{low}, Sca-1^{−}, cKit^{high}, CD34^{+} cells purified from healthy and leukemic mice were stimulated with or without mSCF and then subjected to flow cytometry with phospho-Akt[Ser473] (CD34^{+} myeloid progenitors [MP] versus CD34^{+} leukemic progenitors [LP], p = 0.0478). Right panel is a histogram from a single experiment with the left panel representing mean ± standard error of the mean (SEM) from three experiments.

(B) Mononuclear bone marrow cells (MNBCs) recovered from MLL-AF9 leukemic mice were infected with MSCV-IRES-GFP control (Ctrl) or myr-Akt-expressing retroviruses. Cells from each condition were then treated with vehicle or 10 nM or 100 nM rapamycin and evaluated for numbers of GFP^{+} cells every 2 days using flow cytometry (day 6 *Ctrl versus myr-Akt, vehicle, p = 0.0005; **Ctrl versus myr-Akt, 10 nM rapamycin, p = 0.0008; ***Ctrl versus myr-Akt, 100 nM rapamycin, p = 0.0046; n = 3). Data are represented as the mean ± standard deviation (SD).

(C) GFP^{+} cells treated as described above were analyzed for CD11b expression (*Ctrl versus myr-Akt, vehicle, p < 0.0001; **Ctrl versus myr-Akt, 10 nM rapamycin, p < 0.0001; *** Ctrl versus myr-Akt, 100 nM rapamycin, p < 0.0001; n = 3) or (D) stained with May-Grünwald Giemsa. Data are represented as the mean ± SD.

(E and F) Flow cytometric analysis of control and myr-Akt-infected cells incubated with pHrodo fluorescent-labeled *E. coli* particles. (E) Flow cytometric histogram plot of pHrodo-stained Ctrl versus myr-Akt GFP^{+} cells and (F) graphical representation of three replicates (*Ctrl versus myr-Akt, vehicle, p < 0.0001; **Ctrl versus myr-Akt, 10 nM rapamycin, p < 0.0001; ***Ctrl versus myr-Akt, 100 nM rapamycin, p = 0.0009; n = 3). Data are represented as the mean ± SD.

(G) Flow cytometric analysis of Annexin V expression on Ctrl and myr-Akt-expressing cells (*Ctrl versus myr-Akt, p = 0.0006; n = 3). Data are represented as the mean ± SD.

See also Figure S1.

L-GMPs by assessment of several well-established FoxO target genes. *Cdkn1b (p27)*, *Cited2*, *Ccrn4l*, *Meis1*, *Tmem71*, and *Ccng2* are all activated by FoxOs and were found to be upregulated in L-GMPs compared to GMPs (Figure 2A). *Ccnd1*, *Ccnd2*, *Atm*, and *Sox4*, which are repressed by FoxOs, were documented to be downregulated in L-GMPs (Figure 2A).

Because AKT-mediated phosphorylation of FOXOs leads to nuclear exclusion and subsequent inactivation (Brunet et al., 1999), the nuclear localization of FoxO3 (the dominant FoxO family member active in the murine hematopoietic system; Miyamoto et al., 2007; Yalcin et al., 2008) was evaluated in normal GMPs and L-GMPs by immunofluorescence. FoxO3
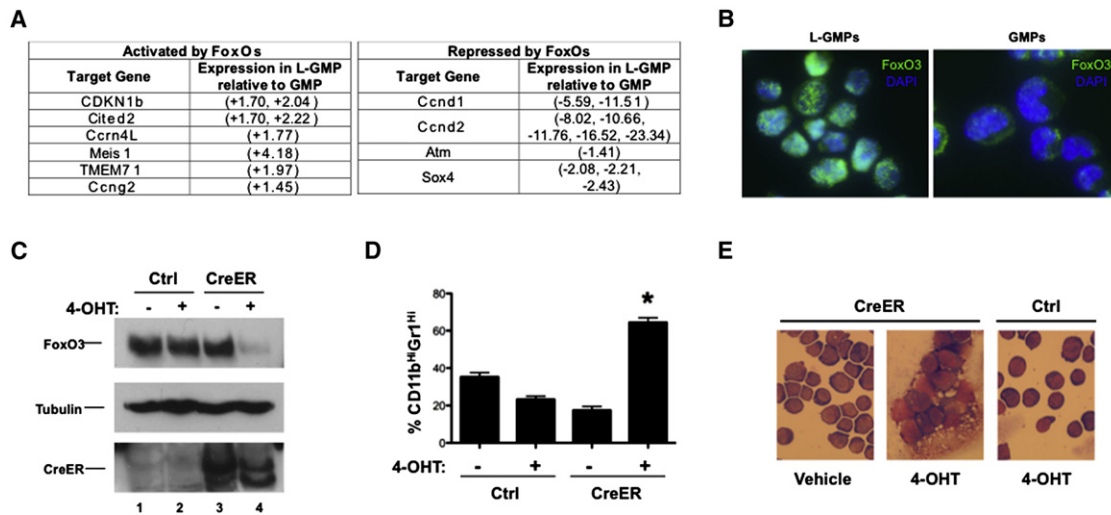
Figure 2. FoxOs Are Active and Suppress Myeloid Maturation in Murine AML Cells

(A) Table of activated (left panel) and repressed (right panel) FoxO target genes differentially expressed between GMP and L-GMP microarray datasets (D-Chip analysis, p = 0.95).

(B) Immunofluorescence of purified lineage^{low}, Sca-1^{-}, cKit^{high}, CD34^{+}, FcgRII/III^{+} cells from healthy and MLL-AF9-induced leukemic mice with FoxO3-specific antibodies (75D8) and DAPI contrast.

(C) Mononuclear bone marrow leukemia cells expressing MLL-AF9 and bearing floxed alleles for *FoxO1*, *FoxO3*, and *FoxO4* (*FoxO1/3/4^{floxed}*;MLL-AF9 cells) were infected with Ctrl or CreER-expressing recombinant retroviruses and then treated with vehicle or 400 nM 4-hydroxytamoxifen (4-OHT) for 4–6 hr. 48–72 hr following treatment, cells from all conditions were subjected to western blotting with FoxO3, Tubulin, and Cre antibodies.

(D) Five days following treatment, Ctrl and CreER cells from each condition were assessed by flow cytometry for CD11b and Gr-1 expression (*CreER + 4-OHT versus CreER + vehicle, Ctrl + vehicle, or Ctrl + 4-OHT, p < 0.0001; n = 3, data represented as the mean ± SEM) and (E) stained with May-Grünwald Giemsa. See also Figure S2.

was predominantly cytoplasmic in GMPs, whereas L-GMPs displayed nuclear localization of FoxO3 (Figures 2B). Collectively, these data suggest that FoxOs are active in L-GMPs but do not exclude that they are also active in other AML cellular subsets.

## Deletion of FoxOs Promotes Myeloid Maturation of Murine AML Cells

Next, we sought genetic evidence for an active role of FoxOs in the maintenance of the differentiation blockade of leukemic cells. BM cells recovered from mice bearing homozygous floxed alleles of *FoxO1, FoxO3*, and *FoxO4* (*FoxO1/3/4^{floxed}*) were transduced with recombinant retroviruses expressing human MLL-AF9. *FoxO1/3/4^{floxed}*;MLL-AF9 leukemic BM cells were then engineered to stably express the CreER fusion protein, thus allowing for inducible excision of *FoxO1/3/4^{floxed}* alleles ex vivo (Figure 2C). *FoxO1/3/4^{floxed}*;MLL-AF9 leukemic cells stably expressing CreER were cultured in the presence and absence of 4-hydroxytamoxifen (4-OHT) and monitored for changes in immunophenotype and morphology. Deletion of *FoxO1/3/4* resulted in increased surface expression of the mature myeloid cell markers CD11b and Gr-1 (Figure 2D and Figure S2A). Ablating *FoxO1/3/4* also induced morphological changes consistent with myeloid maturation (Figure 2E and Figure S2B). The myeloid maturation observed with *FoxO1/3/4* deletion was associated with gene ablation and not Cre expression alone (Figures S2C and S2D). Finally, deletion of *FoxO1/3/4* diminished the ability of *FoxO1/3/4^{floxed}*;MLL-AF9

leukemic cells to form and maintain colonies on supportive stroma (Figures S2E and S2F). Together, these data indicate that *FoxO1/3/4* deficiency promotes myeloid maturation, mirroring the activated Akt phenotype.

Depletion of FOXO3 Promotes Myeloid Maturation and Apoptosis of Human AML Cell Lines

To determine whether FOXO3 is also active in human AML cell lines carrying MLL-AF9 translocations, the cytoplasmic and nuclear fractions of THP-1 and Mono-mac-6 (MM6) cells were evaluated for FOXO3 expression. Similar to our murine model, FOXO3 was nuclear in these human AML cell lines with approximately equal distribution between the two cellular compartments. Furthermore, SKM-1 cells as well as a human acute promyelocytic leukemia (APL) cell line (NB4), neither of which bear MLL translocations, displayed 75% and 86% nuclear FOXO3, respectively, suggesting that FOXO3 may serve comparable biological roles in other forms of AML (Figure 3A).

To determine human AML dependence on FOXOs, we used FOXO3 shRNA in cell lines with MLL-AF9 translocations (MOLM-14, THP-1, MM6, and NOMO-1), APL cell lines (HL-60 and NB4), and AML cell lines that do not carry MLL translocations (SKM-1 and U-937) (Figure 3B and Figure S3A). All eight cell lines expressing FOXO3 shRNA exhibited lower growth rates compared to control shRNA-expressing cells (Figure 3C and Figure S3B). Depletion of FOXO3 resulted in increased CD11b expression (Figure 3D and Figure S3C) and morphological changes consistent with myeloid maturation (Figure 3F and
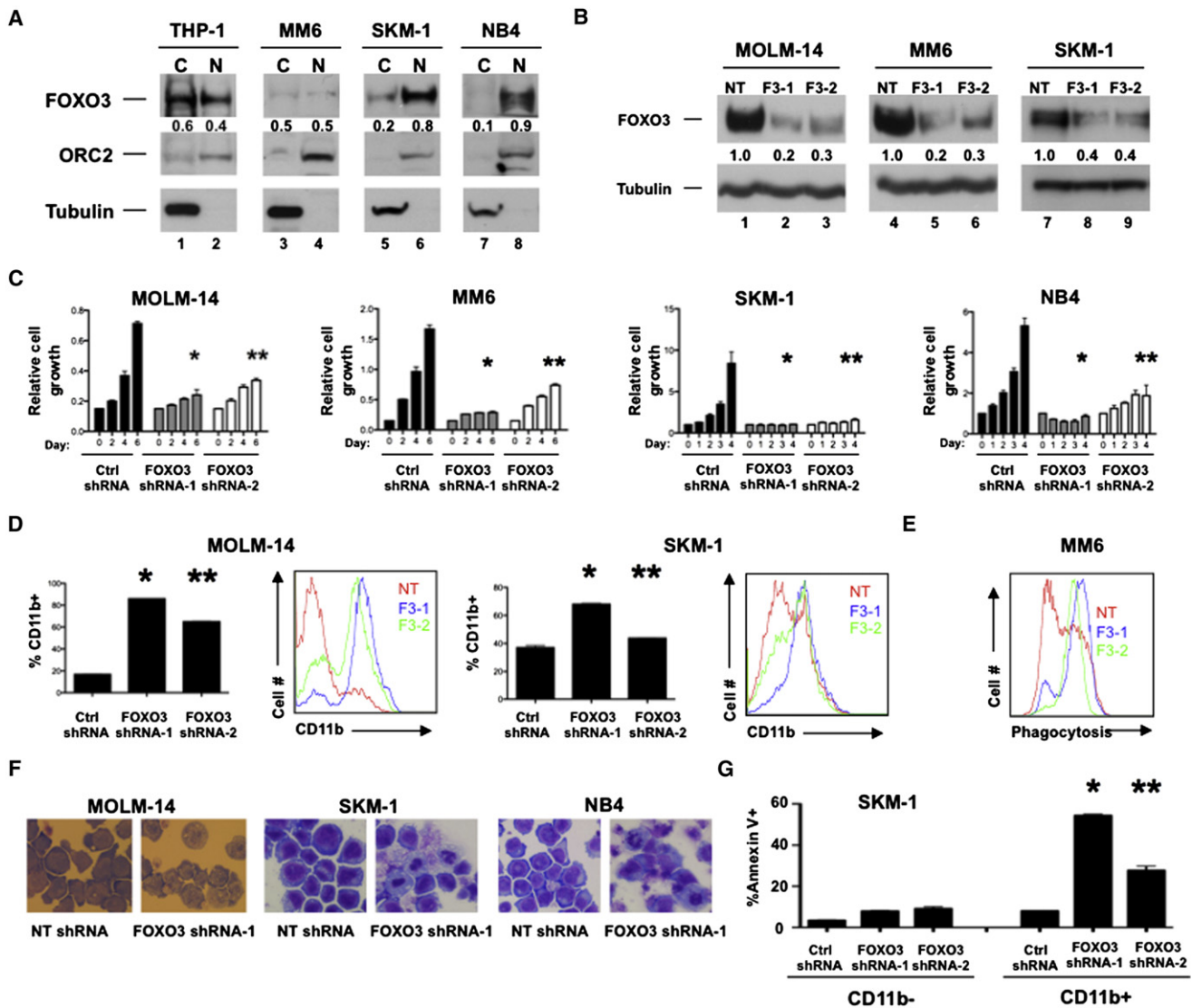
Figure 3. FOXO3 Is Active and Required to Preserve the Immature State of Human AML Cell Lines

(A) THP-1 and Mono-mac-6 (MM6) (both MLL-AF9^{+}) and SKM-1 and NB4 (both MLLAF9^{−}) leukemia cell lines were fractionated into nuclear (N) and cytoplasmic (C) extracts and subjected to western blotting with FOXO3, ORC2 (nuclear), and Tubulin (cytoplasmic) antibodies.

(B) MOLM-14, MM6, and SKM-1 cells were stably transduced with recombinant lentiviruses expressing either nontargeting (NT) or FOXO3 (F3-1 or F3-2) shRNAs. Cells were then subjected to western blotting with FOXO3 and Tubulin antibodies or (C) counted either everyday (SKM-1 and NB4) or every 2 days (MOLM-14 and MM6) following stable expression of designated shRNAs (day 6 MOLM-14, NT versus F3-1, *p = 0.0003; NT versus F3-2, **p < 0.0001; day 6 MM6, NT versus F3-1, *p < 0.0001; NT versus F3-2, **p = 0.0002; day 4 SKM-1, NT versus F3-1, *p = 0.0062; NT versus F3-2, **p = 0.0083; day 4 NB4, NT versus F3-1, *p = 0.0003; NT versus F3-2, **p = 0.0058). Data are represented as the mean ± SD.

(D) Transduced MOLM-14 and SKM-1 cells were analyzed by flow cytometry for human CD11b expression (MOLM-14, NT versus F3-1, *p < 0.0001; NT versus F3-2, **p < 0.0001; SKM-1, NT versus F3-1, *p < 0.0001; NT versus F3-2, **p = 0.0115). Data are represented as the mean ± SD.

(E) Flow cytometric analysis of transduced MM6 cells incubated with pHrodo particles.

(F) May-Grünwald Giemsa staining of transduced MOLM-14, SKM-1, and NB4 cells.

(G) Flow cytometric analysis of transduced SKM-1 cells stained with Annexin V and CD11b (*NT shRNA versus FOXO3 shRNA-1, CD11b^{+}, p < 0.0001; **NT shRNA versus FOXO3 shRNA-2, CD11b^{+}, p = 0.0007; n = 3). Data are represented as the mean ± SD.

NT = NT shRNA, F3-1 = FOXO3 shRNA-1, and F3-2 = FOXO3 shRNA-2; n = 3. See also Figure S3.

Figure S3E). Knockdown of FOXO3 also enhanced the phagocytic capabilities of MOLM-14 and MM6 cells (Figure 3E and Figure S3D). Finally, CD11b^{+} cells expressing FOXO3 shRNAs displayed a marked increase in apoptosis (Figure 3G and Figure S3F). Depletion of FOXO3 did not reduce cell numbers, increase mature myeloid surface markers, or alter the phagocytic properties (Figures S3A, S3B, and S3D) of the BCR-ABL-positive cell line K562.
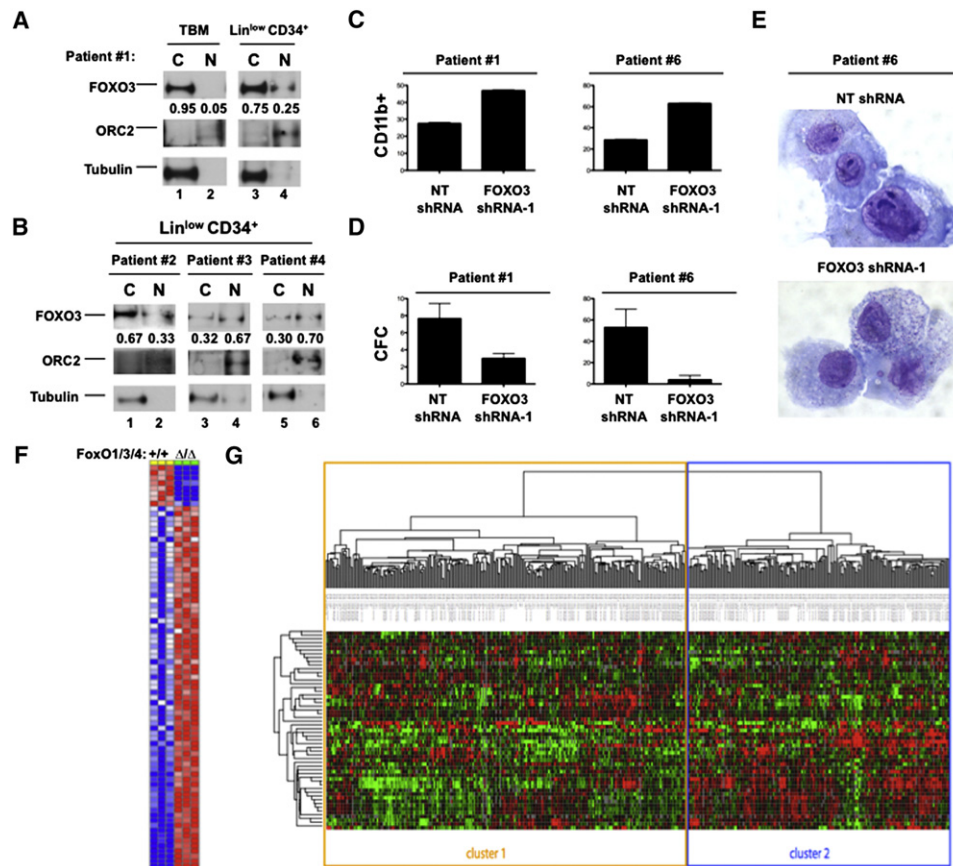
Figure 4. Primary AMLs Derived from Patients Separate into Distinct Clusters of FOXO Activity

(A) BM cells derived from patients with AML were stained with human lineage cocktail and human CD34 (both BD Biosciences), and then lineage^low, CD34^+ cells were isolated by flow cytometry. Nuclear (N) and cytoplasmic (C) extracts of total MNBCs (TBM) and lineage^low, CD34^+ cells were subjected to western blotting with FOXO3, ORC2, and Tubulin antibodies.

(B) Lineage^low, CD34^+ cells from three AML patients analyzed as described above.

(C) Patient samples #1 and #6 were transduced with recombinant lentiviruses expressing either NT shRNA or FOXO3 shRNA-1, then grown in liquid culture for 8 days, and then assessed for CD11b expression. Bar graphs are represented as the mean ± SD.

(D) Transduced patient samples #1 and #6 cells were placed in methylcellulose supplemented with human cytokines. Graph represents the enumeration of colonies formed after 8 days of culture. Data are represented as the mean ± SD.

(E) Transduced cells from patient sample #1 stained with Wright-Giemsa after 8 days of liquid culture.

(F) Gene list comprising the FOXO-specific gene signature generated from comparing the gene expression array data of murine lineage^low, Sca-1^+, cKit^+ (LSK) cells in animals without (+/+) and with (Δ/Δ) FoxO1/3/4 deletion (comprehensive gene set located in Table S1).

(G) Hierarchical cluster analysis based on the overlap of the murine FOXO gene signature stratified over the gene expression array data of 436 individual primary AML samples.

See also Figure S4 and Table S1.

FOXO3 Is Activated in Primary AMLs Derived from Patients

To validate our findings in AML cell lines, the cellular distribution of FOXO3 was examined in primary BM cells derived from nine different AML patients. Biochemical fractionation displayed a wide variation between samples in the nuclear-to-cytoplasmic ratio of FOXO3 (3%–70% nuclear FOXO3) (Figures 4A and 4B; Figures S4A and S4B). Five of the nine samples contained CD34^+ blasts. Fluorescence-activated cell sorting (FACS) isolation of the CD34^+, lineage^low population revealed enrichment for nuclear FOXO3 in comparison with fractionation of the total BM or CD34^−, lineage^high cells (Figure 4A and Figure S4A). Within

these five samples, the overall level of nuclear FOXO3 varied between 10%–70%. Depletion of FOXO3 reduced colony formation in methylcellulose and promoted myeloid maturation (by surface marker expression and morphology) in two samples (Figures 4C–4E).

To determine the global status of FOXO activity in AML, gene expression array data from murine hematopoietic stem cells (HSCs) with and without FoxO1/3/4 (Tothova et al., 2007) were utilized to generate a hematopoietic-specific gene signature of FOXO activity (Figure 4F; Table S1). Using this FoxO target gene set, unsupervised hierarchical clustering analysis of 436 primary AML samples was performed (Bullinger et al., 2004;

Kharas et al., 2010a). The differential expression of FOXO target genes stratified AML into two distinct clusters, strongly suggesting that these clusters reflect two distinct patterns of FOXO activity; cluster 1 AMLs display lower FOXO activity relative to AMLs within cluster 2 (Figure 4G). Consistent with this notion, *FOXO1* and *FOXO3* expression in cluster 2 (higher FOXO activity) is significantly elevated compared to cluster 1 (lower FOXO activity) (p < 0.0001; Figure 7C). Each cluster was significantly represented in nine AML subgroups separated on the basis of defined chromosomal aberrations, indicating that FOXO activation is not restricted to a particular subtype of AML (p < 0.0001; Figure S4C). However, AMLs bearing *FLT3*-ITD mutations (associated with poor prognosis) were underrepresented in the cluster 2 (higher FOXO activity) gene signature (p < 0.0001; Figure S4D). Combined, these analyses extend the importance of FOXOs beyond MLL-AF9+ AMLs and suggest that FOXOs may impact a broad spectrum of myeloid leukemias of various genotypes.

MLL-AF9 Leukemic Burden Is Reduced in the Absence of FoxO1/3/4 In Vivo

To address whether FoxO1/3/4 are essential to maintain MLL-AF9-induced AML in vivo, we used a MLL-AF9 bone marrow transplant (BMT) assay in a mouse bearing homozygous *Lox-P* flanked (floxed) alleles of *FoxO1/3/4* and the interferon-inducible *Mx1-Cre* transgene (*FoxO1/3/4^{floxed}*;*Mx1-Cre$^+$*;MLL-AF9—hereafter Cre$^+$). MLL-AF9-transformed *FoxO1/3/4^{floxed}* BM cells without the *Mx1-Cre* transgene (*FoxO1/3/4^{floxed}*;*Mx1-Cre$^-$*;MLL-AF9—hereafter Cre$^-$) were used as controls. Leukemia cells recovered from primary recipients displaying frank leukemia were transplanted into sublethally irradiated recipients. Fourteen days post-transplant, Cre$^-$ and Cre$^+$ secondary recipients were administered polyinosine-polycytidyline (pI-pC) to induce excision of *FoxO1/3/4* floxed alleles or saline control (Figure 5A). At the first presentation of AML, all mice from each group were euthanized and assessed for leukemic burden as defined by spleen weight and peripheral white blood cell (WBC) counts. Saline- and pI-pC-treated Cre$^-$ and saline-treated Cre$^+$ recipients all developed splenomegaly and leukocytosis (Figures 5B–5D; Figure S5A). In contrast, pI-pC-treated Cre$^+$ transplanted mice retained normal spleen weights and WBC counts (Figures 5B–5D; Figure S5A).

To distinguish whether disrupting FoxO1/3/4 expression eliminated MLL-AF9 leukemia or merely delayed the onset, we evaluated the survival rates of Cre$^-$ and Cre$^+$ recipient mice that were given saline or pI-pC. Blood from recipient mice was analyzed every 4–14 days. Consistent with the prior findings, pI-pC-treated Cre$^+$ mice had lower WBC counts than saline-treated controls (Figure 5D). Regardless of pI-pC treatment, recipient mice transplanted with Cre$^-$ leukemic cells or those transplanted with saline-treated Cre$^+$ cells had similar latencies for AML (Figures 5E and 5F). In contrast, mice transplanted with pI-pC-treated Cre$^+$ leukemic cells (*FoxO1/3/4* deleted) displayed a significantly longer latency. Interestingly, 20% of mice (n = 10) were disease free up to 5 months post-excision. However, despite efficient excision of *FoxO1/3/4* (Figures S5C–S5F), the majority of mice eventually succumbed to leukemia (Figure 5F), the basis for which we subsequently discovered as noted below.

Collectively, these in vivo studies show that one or more of *FoxO1/3/4* support MLL-AF9-induced leukemia.

FoxO1/3/4 Are Required for LIC Function In Vivo

The LIC population represents a small subset of AML cells that retain the ability to give rise to leukemia in recipient mice. Because the L-GMP population of this AML model is enriched for LICs, we first assessed how the deletion of *FoxO1/3/4* affected L-GMP frequency. Specifically, Cre$^+$ recipient mice were administered pI-pC (Δ/Δ) or saline (+/+) 14 days post-transplantation. Seven days following pI-pC treatment, BM cells were analyzed and a reduction in L-GMPs with a concomitant increase of lineage^{high}, CD11b^{hi} myeloid cells was noted (Figures 5G and Figure S5G).

To test whether loss of *FoxO1/3/4* also diminished LIC function, we performed a limit dilution assay. Leukemic BM cells from Cre$^+$ mice 7 days following pI-pC or saline treatment were transplanted into recipients at cell doses of 3×10^2, $\times 10^3$, $\times 10^4$, $\times 10^5$/animal. On day 130 post-transplantation, 17%, 50%, 100%, 100%, respectively (corresponding to the cell doses above), of saline-treated Cre$^+$ (+/+) mice succumbed to AML (LIC frequency = 1:5,314; Figure 5H). In contrast, 0%, 0%, 25%, 100%, respectively, of mice transplanted with pI-pC-treated Cre$^+$ (Δ/Δ) donor cells developed AML (LIC frequency = 1:86,044), an ~16-fold reduction in LIC frequency (Figure 5I). Furthermore, mice transplanted with 300,000 Cre$^+$ (Δ/Δ) cells displayed nearly a 2-fold increase in median survival over mice transplanted with Cre$^+$ (+/+) donor cells (median survival 43 versus 82 days, Figures 5H and 5I), consistent with *FoxO1/3/4* deletion significantly extending the latency of MLL-AF9-positive AML in vivo (n = 4, p = 0.0007). Additionally, mice reconstituted with donor cells from Cre$^+$ (Δ/Δ) mice from Figure 5F displayed an extended latency in comparison with recipients transplanted with donor cells from Cre$^+$ (+/+) leukemic mice in Figure 5F (Figure S5B). Taken together, these data demonstrate that FoxO1/3/4 expression modulates LIC activity in vivo.

Constitutive Activation of Akt Does Not Alter Disease Latency In Vivo

We examined the effects of expressing myr-Akt in MLL-AF9-induced leukemia cells in vivo. BM cells derived from mice transformed with MLL-AF9 were infected with either control or myr-Akt recombinant retroviruses that also express GFP. Following infection, GFP$^+$ cells from each condition were isolated by FACS and separately injected into syngeneic recipients. Mice from all conditions succumbed to AML, and we did not observe any significant difference in latency between control and myr-Akt-expressing AMLs (Figure S5H). The lack of impact on latency was unexpected and caused us to examine whether a mechanism of resistance to Akt activation had emerged.

Inhibition of FOXO3 Results in Activated JNK/c-JUN Signaling

To evaluate the downstream molecular events that regulate myeloid maturation of leukemic cells in response to FOXO inhibition, we examined the status of multiple signaling pathways involved in myeloid differentiation. Phosphorylation of ERK, AKT, and c-JUN was assessed upon shRNA-mediated inhibition
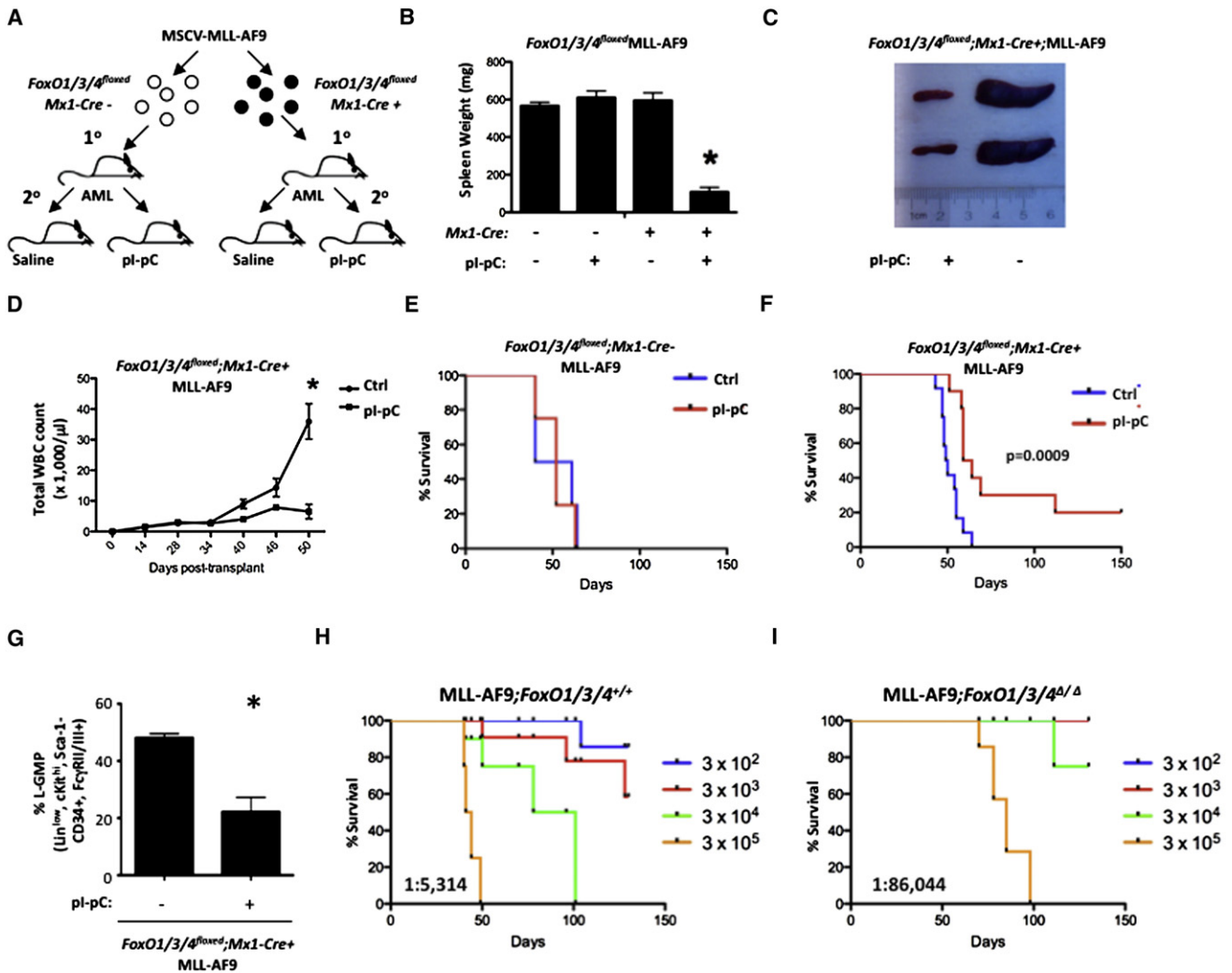
Figure 5. Deletion of FoxO Transcription Factors Suppresses MLL-AF9-Induced Leukemia In Vivo

(A) Experimental scheme used in Figures 5B–5H where MLL-AF9+ *FoxO1/3/4floxed* murine bone marrow (BM) cells recovered from a leukemic primary recipient mouse carrying the *Mx1-Cre* transgene (Cre+) or not (Cre−) were transplanted into recipient mice. Cre+ and Cre− mice were administered saline or pI-pC and then all mice from each Cre condition were assessed for leukemic burden (day 29 for Cre− and day 39 for Cre+).

(B) Mean spleen weight of Cre+ (pI-pC) versus Cre+ (saline) (p < 0.0001; n = 4). Data represented as the mean ± SEM.

(C) Gross anatomical view of spleens recovered from Cre+ mice administered pI-pC (right) or saline (left).

(D) WBC analysis of peripheral blood collected every 4–14 days post-transplant from Cre+ saline- and pI-pC-treated mice (n = 4).

(E and F) Kaplan-Meier survival curve analysis of mice transplanted and treated as described above (E: Cre−, p = 0.6899; n = 6 and F: Cre+, p = 0.0009; n = 10).

(G) Leukemic BM cells isolated from Cre+ mice administered saline or pI-pC 7 days earlier were analyzed for the mean proportion ± SEM of L-GMPs (lineage^low, Sca-1−, cKit^high, CD34+, FcgRII/III+, p = 0.039; n = 3).

(H and I) Leukemic BM cells isolated from Cre+ mice administered saline (H) or pI-pC (I) 7 days earlier were transplanted into tertiary recipients at various cell numbers: 300 (n = 6), 3,000 (n = 6), 30,000 (n = 4), and 300,000 (n = 4). Kaplan-Meier analysis of animals that developed leukemia is shown. LIC frequencies were calculated using poisson statistics (H: LICfreq^+/+ = 1:5,314 and I: LICfreq^Δ/Δ = 1: 86,044).

See also Figure S5.

of FOXO3 expression in MOLM-14 and SKM-1 cells. Although FOXO3 depletion did not have a substantial effect on AKT or ERK phosphorylation, serine 63 phosphorylation within c-JUN (pc-JUN^Ser63) was elevated in both cell lines (Figure S6A). The c-JUN oncogene is a member of the AP-1 family of transcription factors that is phosphorylated and activated by the stress-activated kinase SAPK/JNK (hereafter JNK) (Dérijard et al., 1994; Hibi et al., 1993). Under various forms of stress, JNK is phosphorylated at threonine 183/tyrosine 185 (pJNK^Thr183/Tyr185) (Dérijard et al., 1994). Depletion of FOXO3 resulted in substantial increases in pJNK^Thr183/Tyr185, pc-JUN^Ser63, and total c-JUN (Figure 6A and Figure S6B). Enforced expression of myr-Akt in murine MLL-AF9-expressing AML cells led to increased phosphorylation of FoxO3^Ser256 (pFoxO3^Ser256) as well as increases in pJnk^Thr183/Tyr185, pc-Jun^Ser63, and total c-Jun (Figure 6D).
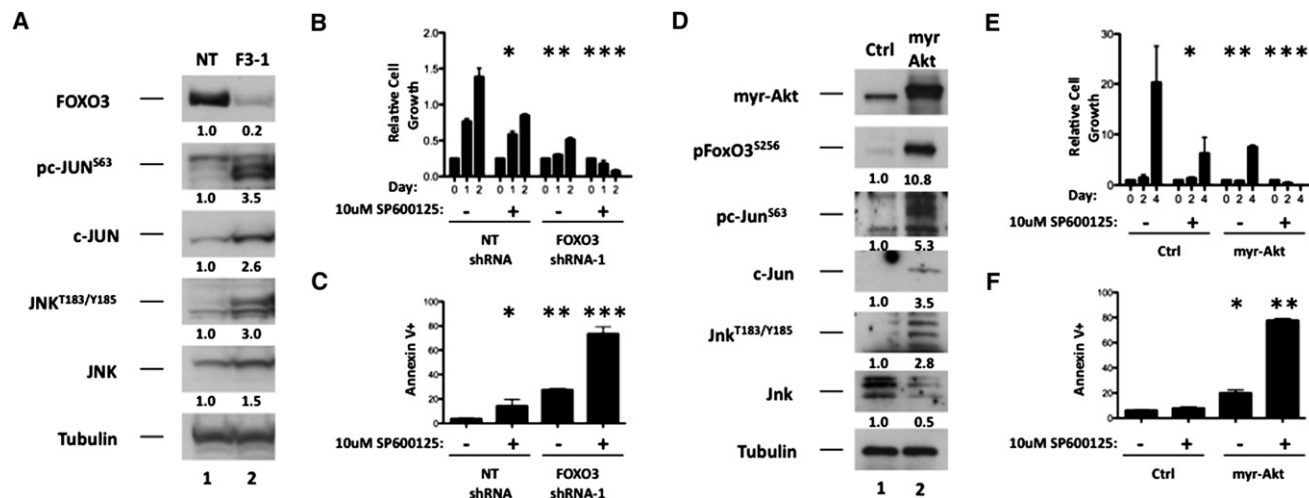
Figure 6. The JNK/c-JUN Signaling Pathway Antagonizes Maturation and Apoptosis Mediated by FOXO Inhibition in AML

(A) MOLM-14 cells stably expressing either nontargeting (NT) or FOXO3 (FOXO3-1) shRNA were subjected to western blotting with antibodies that specifically recognize FOXO3, c-JUN, JNK, Tubulin, or the phosphorylated forms of c-JUN (pc-JUN^{S63}) and JNK (pJNK$^{T183/Y185}$).

(B and C) MOLM-14 cells stably expressing nontargeting (NT) or FOXO3 (F3-1) shRNA were treated with 10 μM SP600125 (JNK inhibitor) or vehicle. Forty-eight hours later, cells from each condition were assessed for cell number (B, NT [vehicle] versus NT [SP600125], *p = 0.0095, NT [SP600125] versus F3-1 [vehicle], **p = 0.0008, F3-1 [vehicle] versus F3-1 [SP600125], ***p < 0.0001) and Annexin V staining (C, NT [vehicle] versus NT [SP600125], *p = 0.0282, NT [SP600125] versus F3-1 [vehicle], **p = 0.0133, F3-1 [vehicle] versus F3-1 [SP600125], ***p = 0.0002). Data are represented as the mean ± SD.

(D) Control and myr-Akt-expressing MLL-AF9^{+} leukemia BM cells were subjected to western blotting with FoxO3, c-Jun, Jnk, Tubulin, or the phosphorylated forms of FoxO3 (pFoxO3^{S256}), c-Jun (pc-JUN^{S63}), and Jnk (pJnk$^{T183/Y185}$) antibodies.

(E and F) Control and myr-Akt-expressing MLL-AF9^{+} leukemia BM cells were treated with 10 μM SP600125 (JNK inhibitor) or vehicle. Forty-eight hours after treatment, cells from each condition were assessed for cell number (E, Ctrl [vehicle] versus Ctrl [SP600125], *p = 0.0373, Ctrl [vehicle] versus myr-Akt [vehicle], **p = 0.0381, myr-Akt [vehicle] versus myr-Akt [SP600125], ***p < 0.0001) and Annexin V staining (F, Ctrl [SP600125] versus myr-Akt [vehicle], *p = 0.0011, myr-Akt [vehicle] versus myr-Akt [SP600125], **p < 0.0001). Data are represented as the mean ± SD.

See also Figure S6.

Pharmacological Inhibition of JNK Cooperates with FOXO Inhibition to Induce AML Cell Death

We then tested whether JNK/c-JUN signaling has a functional impact on cellular events induced by AKT and FOXO signaling. We combined a pan-JNK inhibitor (SP600125, Calbiochem) with either FOXO3 depletion or myr-Akt expression and evaluated the growth, differentiation, and survival of AML cells. Treatment of control-infected MOLM-14-, SKM-1-, or MLL-AF9-expressing murine leukemia cells with SP600125 caused a modest but significant decrease in cell growth and a mild increase in mature myeloid surface marker expression and apoptosis (Figures 6B, 6C, 6E, and 6F; Figures S6C–S6E). As seen previously, depletion of FOXO3 or myr-Akt resulted in significant decreases in cell growth and increases in mature myeloid surface marker expression and apoptosis (Figures 6C and 6F; Figures S6C–S6E). Notably, the combination of SP600125 with either FOXO3 depletion or myr-Akt expression led to a significant decrease in cell growth and increases in apoptosis and mature myeloid surface marker expression compared to FOXO3 shRNA, myr-Akt expression, or SP600125 treatment alone (Figures 6B, 6C, 6E and 6F; Figures S6D–S6F). Furthermore, SP600125 combined with myr-Akt resulted in morphological changes associated with myeloid differentiation (Figure S6F). Together, these data suggest that FOXO3 inhibition or AKT activation in AML results in JNK/c-JUN pathway activation mitigating the antileukemic properties of FOXO3 inhibition or AKT activation.

c-JUN Activity Is Elevated in AMLs with Diminished FOXO Activity

As JNK/c-JUN signaling was activated in response to FOXO inhibition (directly or via Akt activation), we examined whether activation of this pathway was also initiated in vivo. Analyzing the phosphorylation status of c-Jun in *FoxO1/3/4^{floxed}* (saline) and *FoxO1/3/4$^{Δ/Δ}$* (pI-pC) leukemic BM cells recovered from mice (Figure 5F) with AML, we observed increased pc-Jun^{Ser63} in 75% of mice that died of AML despite efficient deletion of *FoxO1/3/4* (Figure 7A and Figures S5C–S5F). We also evaluated the phosphorylation status of BM cells derived from control and myr-Akt-expressing leukemic mice from Figure S5H. Leukemic BM from four mice that succumbed to AML expressing MLL-AF9 and myr-Akt displayed elevated pc-Jun^{Ser63} compared to control leukemic BM (Figure 7B). Furthermore, all four myr-Akt-expressing AMLs displayed increases in pFoxO3^{Ser256}, confirming that myr-Akt was inhibiting FoxO in these tumors (Figure 7B).

To get a broader understanding of the relationship between FOXO inhibition and JNK/c-JUN activation in human AML, the expression of *c-JUN* was determined in the gene expression array dataset generated from 436 primary AML patient samples. *c-JUN* expression inversely correlated with FOXO activity and *FOXO1* and *FOXO3* expression (p < 0.0001; Figure 7C). Collectively, these data demonstrate that inhibition of the AKT/FOXO signaling pathway preserves the immature phenotype and the
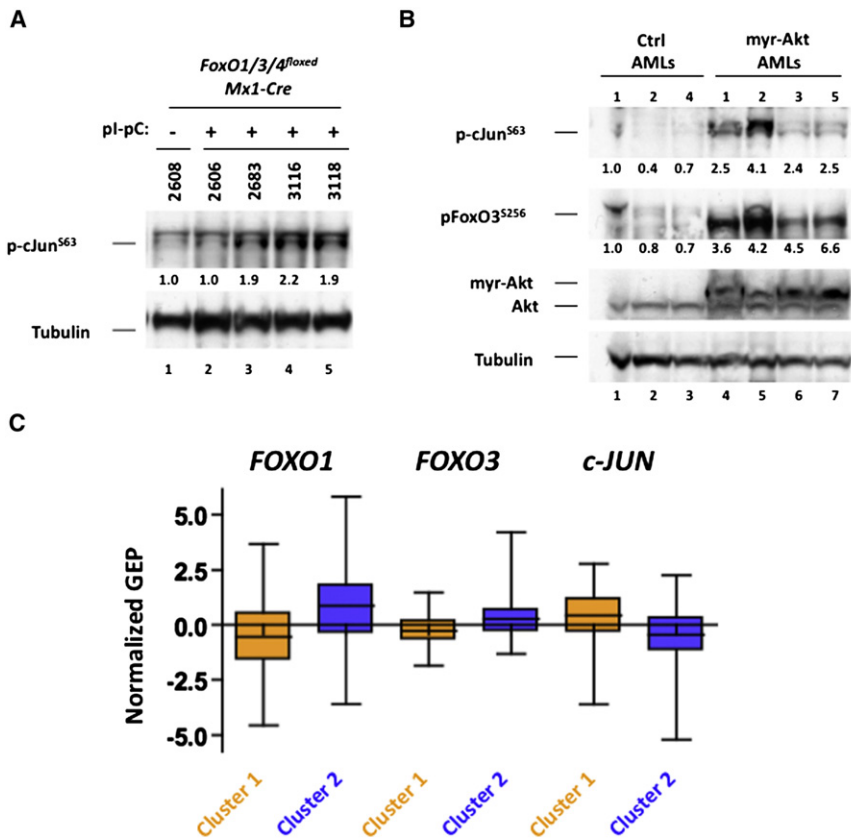
Figure 7. c-JUN Activity Is Upregulated in AMLs Displaying Constitutive AKT Activation or FOXO Inhibition

(A) BM cells recovered from mice that succumbed to MLL-AF9-induced AML (refer to Figure 5F) that were wild-type or null for *FoxO1/3/4* were subjected to western blotting with pc-Jun^{S63} and Tubulin antibodies.

(B) BM cells recovered from mice that succumbed to control or myr-Akt-expressing MLL-AF9-induced AML (refer to Figure S5G) were subjected to western bloting with antibodies that recognize Akt, Tubulin, or the phosphorylated forms of FoxO3 (pFoxO3^{S256}) or c-Jun (pc-Jun^{S63}) antibodies.

(C) Mean expression levels of *FOXO1*, *FOXO3*, and *c-JUN* in the FOXO signature-based, hierarchical cluster-defined primary AML sample groups (p < 0.0001; see Figure 4G). Data are represented in a box plot with whiskers.

leukemia-initiating properties of various AML subtypes. These data also suggest that activation of the JNK/c-JUN pathway represents a common mechanism by which AML tolerates the deregulation of FOXO/AKT signaling and offers a therapeutic opportunity of targeting deregulated JNK/c-JUN signaling in FOXO/AKT-deregulated AML.

DISCUSSION

In many human cancers, the serine/threonine kinase AKT promotes tumorigenesis by phosphorylating and inactivating targets that antagonize malignant growth, such as the FOXO family of transcription factors. We have identified an unexpected, yet crucial role of the FOXO signaling arm of the AKT pathway in the maintenance of the differentiation blockade in AML. We observed that Akt is repressed and FoxO1/3/4 are active in the MLL-AF9 AML cell fraction most highly enriched for LIC activity. Further, enforced activation of Akt or deletion of its canonical downstream targets, *FoxO1, FoxO3*, and *FoxO4* (*FoxO1/3/4*—thought to be tumor suppressors), decrease leukemic growth and maintenance in vitro by promoting myeloid maturation and apoptosis. Ablation of *FoxO1/3/4* in vivo reduced disease burden, diminished LIC function, and extended the life span of animals transplanted with MLL-AF9-positive AML. We confirmed the clinical relevance of our findings by demonstrating that FOXOs are active in primary samples derived from AML patients.

We have also identified a mechanism of resistance to inhibiting FOXOs. Leukemias that persisted despite *FoxO1/3/4* deletion or constitutive Akt activation exhibited c-Jun activation. Pharmacological inhibition of JNK augmented the myeloid maturation and apoptotic effects of Akt activation or FOXO inhibition. These data were supported by patient data where we noted that AML samples with reduced FOXO activity had increased expression of *c-JUN*. Taken together, the data suggest an inverse correlation of FOXO and JNK/c-JUN activation in AML, and that whereas FOXO depletion can induce a therapeutic differentiation of AML cells, increased JNK/c-JUN activity can render cells insensitive to FOXO loss. A combination of reduced FOXO and JNK/c-JUN activation may provide a particularly potent approach to AML.

The previously unrecognized relationship whereby blocking FOXO activity via direct inhibition or Akt activation activates JNK/c-JUN signaling is quite distinctive from prior reports that AKT inhibits JNK by inhibiting the JNK-activating kinase ASK1 (Kim et al., 2001). Also, others noted that JNK can regulate FOXOs, particularly FOXO4, but we are unaware of prior evidence that FOXOs can inhibit JNK signaling (Essers et al., 2004; Wang et al., 2005). Our data suggest that this relationship of AKT/FOXOs to JNK/c-JUN is associated with AML surviving the activation of Akt and/or inhibition of FOXOs. These findings provide a rationale for considering JNK inhibition in antileukemic therapy.

It is not clear why we observed divergence between the results of Akt activation and FOXO inhibition on leukemia outcomes in vivo. However, it may be that some growth-promoting activities of Akt (such as activation of mTorc1 or inactivation of Gsk-3β) may provide countervailing signals in vivo that abrogate the effects of FoxO inhibition (Lee et al., 2010; Wang et al., 2008; Yilmaz et al., 2006).

The genetic and molecular heterogeneity of AML has made the development of universal targeted therapies cumbersome and

relatively unsuccessful. The broad bifurcation we have observed of AMLs based on their AKT, FOXO, and c-JUN signaling coupled with the impact that altering these pathways has on leukemia-initiating cells suggests a possible therapeutic opportunity for the development of more widely acting antileukemic agents.

EXPERIMENTAL PROCEDURES

Plasmid and Mouse Generation
The MSCV-MLL-AF9 construct was a kind gift of Dr. S.A. Armstrong (Children's Hospital of Boston—CHOB). The MSCV-IRES-GFP-myr-Akt construct was kindly provided by Dr. K. Gritsman (Dana-Farber Cancer Institute) and Dr. Michael G. Kharas (CHOB). The MSCV-puro-CreER plasmid was kindly donated by Dr. D. Kalaitzidis (CHOB). The expression plasmid carrying the LSL-hCD34 was kindly donated by Dr. M. Milsom (Heidelberg University). The *FoxO1/3/4^floxed;Mx1-Cre^+* mice were generated previously (Paik et al., 2007; Tothova et al., 2007).

AML Patient Samples
BM aspirates from patients with AML were collected under a protocol approved by the institutional review board (IRB) of Massachusetts General Hospital. Ficoll density gradient was then used to recover viable mononuclear cells from BM aspirates.

MLL-AF9 Retroviral Bone Marrow Transplantation Assay
Both *FoxO1/3/4^floxed;Mx1-Cre^+* and *FoxO1/3/4^floxed;Mx1-Cre^−* mice were administered 150 mg/kg 5-flurouracil (5-FU, Sigma). Recovered mononuclear bone marrow cells (MNBCs) were transduced with recombinant MLL-AF9-expressing retroviruses and transplanted into lethally irradiated F1 FVB/C57/Bl6 mice. Recipient mice developed leukemia within 70–80 days with a median survival of 77 days. MNBCs recovered from leukemic mice were then transplanted into secondary sublethally irradiated recipients. Fourteen days after transplant, secondary recipients were administered intraperitoneally three doses of saline or 12.5 mg/kg pI-pC (Amersham) every 2 days. Mice were then monitored for external (i.e., moribund) and internal (white blood cell counts) signs of leukemia.

Flow Cytometry and Antibodies
MNBCs were stained with a lineage cocktail comprised of antibodies targeting CD3, CD4, CD8, CD19, B220, Gr-1, Ter119, and IL-7Rα. MNBCs were also stained with antibodies targeting cKit, Sca-1, FcγRII/III, and CD34. L-GMP and GMP populations were analyzed and sorted with a FACSAria instrument (Becton Dickinson). For phosphoflow experiments, lineage^low cells were sorted and stained with cKit and CD34 antibodies in combination with phospho-AKT^Ser473, phospho-AKT^Thr308, or phospho-S6^Ser235/236 antibodies and then analyzed on a FACSAria. Primary AML patient BM cells were stained with human CD34 and lineage cocktail. Antibody information including company, clone, and dilution factor are listed in Table S2.

Cell Death Assays
Cells were stained with Annexin V and 7-AAD according to the manufacturer instructions (BD Biosciences) to assess levels of apoptosis. Where indicated, cell death was also evaluated with Trypan Blue staining (Cellgro).

Phagocytosis Assay
Phagocytosis was assessed using a pHrodo BioParticles Conjugates for Phagocytosis Kit (Invitrogen). Assays were performed according to the manufacturer's instructions.

Indirect Immunofluorescence
Cytospins of purified L-GMPs and GMPs were fixed with PFA and permeabilized with methanol. Processed cells were then subjected to staining with FOXO3 (75D8) antibodies. Cells were then incubated with an anti-rabbit FITC-conjugated secondary antibody (1:2000; Sigma). Cells were also stained with DAPI to visualize nuclei and visualized under 100× magnification using a Nikon fluorescence microscope.

Cell Fractionation
Cells were resuspended in hypotonic buffer containing a mild detergent to rupture cellular membrane. Recovered nuclei lysed in a hypertonic solution and cytoplasmic fractions were subjected to western blotting with the corresponding antibodies.

Cell Morphology Staining
Cells from respective conditions were stained first with May-Grünwald dye and then Giemsa stain (Sigma). Alternatively, cells were permeabilized and stained in 100% Wright-Giemsa stain and then stained with 20% Wright-Giemsa/80%.

Colony Assays
Murine myeloid colony assays were plated in M3434 cytokine-enriched methylcellulose according to manufacturer's instructions (Stem Cell Technologies). Human myeloid colony assays were plated in H4034 cytokine-enriched methylcellulose according to manufacturer's instructions (Stem Cell Technologies). For CAFC assays, murine leukemia cells were cocultured on OP9 stroma cells for 7–14 days.

Statistical Analyses
Log-rank (Mantel-Cox) test was used to determine p values for all Kaplan-Meier survival curve analyses. Unpaired, two-tailed Student's t tests were used for all analyses comparing two experimental groups. Poisson statistics was used to determine the LIC frequency in vivo in Figures 5H and 5I as well as in vitro in Figures S2E and S2F.

Additional experimental details can be found in the Extended Experimental Procedures.

SUPPLEMENTAL INFORMATION

Supplemental Information includes Extended Experimental Procedures, six figures, and two tables and can be found with this article online at doi:10.1016/j.cell.2011.07.032.

ACKNOWLEDGMENTS

REFERENCES

Alessi, D.R., Andjelkovic, M., Caudwell, B., Cron, P., Morrice, N., Cohen, P., and Hemmings, B.A. (1996). Mechanism of activation of protein kinase B by insulin and IGF-1. EMBO J. *15*, 6541–6551.

Altomare, D.A., and Testa, J.R. (2005). Perturbations of the AKT signaling pathway in human cancer. Oncogene *24*, 7455–7464.

Arden, K.C. (2006). Multiple roles of FOXO transcription factors in mammalian cells point to multiple roles in cancer. Exp. Gerontol. *41*, 709–717.

Armstrong, S.A., Golub, T.R., and Korsmeyer, S.J. (2003). MLL-rearranged leukemias: insights from gene expression profiling. Semin. Hematol. *40*, 268–273.

Brunet, A., Bonni, A., Zigmond, M.J., Lin, M.Z., Juo, P., Hu, L.S., Anderson, M.J., Arden, K.C., Blenis, J., and Greenberg, M.E. (1999). Akt promotes cell survival by phosphorylating and inhibiting a Forkhead transcription factor. Cell *96*, 857–868.

Bullinger, L., Döhner, K., Bair, E., Fröhling, S., Schlenk, R.F., Tibshirani, R., Döhner, H., and Pollack, J.R. (2004). Use of gene-expression profiling to identify prognostic subclasses in adult acute myeloid leukemia. N. Engl. J. Med. *350*, 1605–1616.

Burgering, B.M., and Coffer, P.J. (1995). Protein kinase B (c-Akt) in phospha-tidylinositol-3-OH kinase signal transduction. Nature *376*, 599–602.

Cross, D.A., Alessi, D.R., Cohen, P., Andjelkovich, M., and Hemmings, B.A. (1995). Inhibition of glycogen synthase kinase-3 by insulin mediated by protein kinase B. Nature *378*, 785–789.

Dash, A., and Gilliland, D.G. (2001). Molecular genetics of acute myeloid leukaemia. Best Practice & Research *14*, 49–64.

Datta, S.R., Dudek, H., Tao, X., Masters, S., Fu, H., Gotoh, Y., and Greenberg, M.E. (1997). Akt phosphorylation of BAD couples survival signals to the cell-intrinsic death machinery. Cell *91*, 231–241.

del Peso, L., González-García, M., Page, C., Herrera, R., and Nuñez, G. (1997). Interleukin-3-induced phosphorylation of BAD through the protein kinase Akt. Science *278*, 687–689.

Dérijard, B., Hibi, M., Wu, I.H., Barrett, T., Su, B., Deng, T., Karin, M., and Davis, R.J. (1994). JNK1: a protein kinase stimulated by UV light and Ha-Ras that binds and phosphorylates the c-Jun activation domain. Cell *76*, 1025–1037.

Döhner, H., Estey, E.H., Amadori, S., Appelbaum, F.R., Büchner, T., Burnett, A.K., Dombret, H., Fenaux, P., Grimwade, D., Larson, R.A., et al; European LeukemiaNet. (2010). Diagnosis and management of acute myeloid leukemia in adults: recommendations from an international expert panel, on behalf of the European LeukemiaNet. Blood *115*, 453–474.

Essers, M.A., Weijzen, S., de Vries-Smits, A.M., Saarloos, I., de Ruiter, N.D., Bos, J.L., and Burgering, B.M. (2004). FOXO transcription factor activation by oxidative stress mediated by the small GTPase Ral and JNK. EMBO J. *23*, 4802–4812.

Fröhling, S., Scholl, C., Gilliland, D.G., and Levine, R.L. (2005). Genetics of myeloid malignancies: pathogenetic and clinical implications. J. Clin. Oncol. *23*, 6285–6295.

Fu, Z., and Tindall, D.J. (2008). FOXOs, cancer and regulation of apoptosis. Oncogene *27*, 2312–2319.

Gallay, N., Dos Santos, C., Cuzin, L., Bousquet, M., Simmonet Gouy, V., Chaussade, C., Attal, M., Payrastre, B., Demur, C., and Récher, C. (2009). The level of AKT phosphorylation on threonine 308 but not on serine 473 is associated with high-risk cytogenetics and predicts poor overall survival in acute myeloid leukemia. Leukemia *23*, 1029–1038.

Guertin, D.A., Stevens, D.M., Thoreen, C.C., Burds, A.A., Kalaany, N.Y., Moffat, J., Brown, M., Fitzgerald, K.J., and Sabatini, D.M. (2006). Ablation in mice of the mTORC components raptor, rictor, or mLST8 reveals that mTORC2 is required for signaling to Akt-FOXO and PKCalpha, but not S6K1. Dev. Cell *11*, 859–871.

Hibi, M., Lin, A., Smeal, T., Minden, A., and Karin, M. (1993). Identification of an oncoprotein- and UV-responsive protein kinase that binds and potentiates the c-Jun activation domain. Genes Dev. *7*, 2135–2148.

Inoki, K., Li, Y., Zhu, T., Wu, J., and Guan, K.L. (2002). TSC2 is phosphorylated and inhibited by Akt and suppresses mTOR signalling. Nat. Cell Biol. *4*, 648–657.

Kharas, M.G., Lengner, C.J., Al-Shahrour, F., Bullinger, L., Ball, B., Zaidi, S., Morgan, K., Tam, W., Paktinat, M., Okabe, R., et al. (2010a). Musashi-2 regulates normal hematopoiesis and promotes aggressive myeloid leukemia. Nat. Med. *16*, 903–908.

Kharas, M.G., Okabe, R., Ganis, J.J., Gozo, M., Khandan, T., Paktinat, M., Gilliland, D.G., and Gritsman, K. (2010b). Constitutively active AKT depletes hematopoietic stem cells and induces leukemia in mice. Blood *115*, 1406–1415.

Kim, A.H., Khursigara, G., Sun, X., Franke, T.F., and Chao, M.V. (2001). Akt phosphorylates and negatively regulates apoptosis signal-regulating kinase 1. Mol. Cell. Biol. *21*, 893–901.

Kops, G.J., de Ruiter, N.D., De Vries-Smits, A.M., Powell, D.R., Bos, J.L., and Burgering, B.M. (1999). Direct control of the Forkhead transcription factor AFX by protein kinase B. Nature *398*, 630–634.

Krivtsov, A.V., Twomey, D., Feng, Z., Stubbs, M.C., Wang, Y., Faber, J., Levine, J.E., Wang, J., Hahn, W.C., Gilliland, D.G., et al. (2006). Transformation from committed progenitor to leukaemia stem cell initiated by MLL-AF9. Nature *442*, 818–822.

Lee, J.Y., Nakada, D., Yilmaz, O.H., Tothova, Z., Joseph, N.M., Lim, M.S., Gilliland, D.G., and Morrison, S.J. (2010). mTOR activation induces tumor suppressors that inhibit leukemogenesis and deplete hematopoietic stem cells after Pten deletion. Cell Stem Cell *7*, 593–605.

Miyamoto, K., Araki, K.Y., Naka, K., Arai, F., Takubo, K., Yamazaki, S., Matsuoka, S., Miyamoto, T., Ito, K., Ohmura, M., et al. (2007). Foxo3a is essential for maintenance of the hematopoietic stem cell pool. Cell Stem Cell *1*, 101–112.

Naka, K., Hoshii, T., Muraguchi, T., Tadokoro, Y., Ooshio, T., Kondo, Y., Nakao, S., Motoyama, N., and Hirao, A. (2010). TGF-beta-FOXO signalling maintains leukaemia-initiating cells in chronic myeloid leukaemia. Nature *463*, 676–680.

Nicholson, K.M., and Anderson, N.G. (2002). The protein kinase B/Akt signalling pathway in human malignancy. Cell. Signal. *14*, 381–395.

Paik, J.H., Kollipara, R., Chu, G., Ji, H., Xiao, Y., Ding, Z., Miao, L., Tothova, Z., Horner, J.W., Carrasco, D.R., et al. (2007). FoxOs are lineage-restricted redundant tumor suppressors and regulate endothelial cell homeostasis. Cell *128*, 309–323.

Park, S., Chapuis, N., Tamburini, J., Bardet, V., Cornillet-Lefebvre, P., Willems, L., Green, A., Mayeux, P., Lacombe, C., and Bouscary, D. (2010). Role of the PI3K/AKT and mTOR signaling pathways in acute myeloid leukemia. Haematologica *95*, 819–828.

Sancak, Y., Thoreen, C.C., Peterson, T.R., Lindquist, R.A., Kang, S.A., Spooner, E., Carr, S.A., and Sabatini, D.M. (2007). PRAS40 is an insulin-regulated inhibitor of the mTORC1 protein kinase. Mol. Cell *25*, 903–915.

Santamaría, C.M., Chillón, M.C., García-Sanz, R., Pérez, C., Caballero, M.D., Ramos, F., de Coca, A.G., Alonso, J.M., Giraldo, P., Bernal, T., et al. (2009). High FOXO3a expression is associated with a poorer prognosis in AML with normal cytogenetics. Leuk. Res. *33*, 1706–1709.

Tamburini, J., Elie, C., Bardet, V., Chapuis, N., Park, S., Broët, P., Cornillet-Lefebvre, P., Lioure, B., Ugo, V., Blanchet, O., et al. (2007). Constitutive phosphoinositide 3-kinase/Akt activation represents a favorable prognostic factor in de novo acute myelogenous leukemia patients. Blood *110*, 1025–1028.

Tothova, Z., Kollipara, R., Huntly, B.J., Lee, B.H., Castrillon, D.H., Cullen, D.E., McDowell, E.P., Lazo-Kallanian, S., Williams, I.R., Sears, C., et al. (2007). FoxOs are critical mediators of hematopoietic stem cell resistance to physiologic oxidative stress. Cell *128*, 325–339.

Wang, M.C., Bohmann, D., and Jasper, H. (2005). JNK extends life span and limits growth by antagonizing cellular and organism-wide responses to insulin signaling. Cell *121*, 115–125.

Wang, Z., Smith, K.S., Murphy, M., Piloto, O., Somervaille, T.C., and Cleary, M.L. (2008). Glycogen synthase kinase 3 in MLL leukaemia maintenance and targeted therapy. Nature *455*, 1205–1209.

Yalcin, S., Zhang, X., Luciano, J.P., Mungamuri, S.K., Marinkovic, D., Vercherat, C., Sarkar, A., Grisotto, M., Taneja, R., and Ghaffari, S. (2008). Foxo3 is essential for the regulation of ataxia telangiectasia mutated and oxidative stress-mediated homeostasis of hematopoietic stem cells. J. Biol. Chem. *283*, 25692–25705.

Yilmaz, O.H., Valdez, R., Theisen, B.K., Guo, W., Ferguson, D.O., Wu, H., and Morrison, S.J. (2006). Pten dependence distinguishes haematopoietic stem cells from leukaemia-initiating cells. Nature *441*, 475–482.